doi.org/10.26434/chemrxiv.12408548.v1

Peptidyl Acyloxymethyl Ketones as Activity-Based Probes for the Main Protease of SARS-CoV-2

Merel Van de Plassche, Marta Barniol-Xicota, Steven Verhelst

Submitted date: 02/06/2020 • Posted date: 03/06/2020

Citation information: Van de Plassche, Merel; Barniol-Xicota, Marta; Verhelst, Steven (2020): Peptidyl Acyloxymethyl Ketones as Activity-Based Probes for the Main Protease of SARS-CoV-2. ChemRxiv. Preprint. https://doi.org/10.26434/chemrxiv.12408548.v1

The global pandemic caused by SARS-CoV-2 calls for a fast development of antiviral drugs against this particular coronavirus. Chemical tools to facilitate inhibitor discovery as well as detection of target engagement by hit or lead compounds from high throughput screens are therefore in urgent need. We here report novel, selective activity-based probes that enable detection of the SARS-CoV-2 main protease. The probes are based on acyloxymethyl ketone reactive electrophiles combined with a peptide sequence including non-natural amino acids that targets the non-primed site of the main protease substrate binding cleft. They are the first activity-based probes for the main protease of coronaviruses and display target labeling within in a human proteome without background. We expect that these reagents will be useful in the drug development pipeline, not only for the current SARS-CoV-2, but also for other coronaviruses.

SUPPORTING INFORMATION

Peptidyl Acyloxymethyl Ketones as Activity-Based Probes for the Main Protease of SARS-CoV-2

Merel A. T. van de Plassche,[1#] Marta Barniol-Xicota,[1#] and Steven H. L. Verhelst[*, 1,2]

[1] KU Leuven, Department of Cellular and Molecular Medicine, Laboratory of Chemical Biology, Herestr. 49, 3000 Leuven, Belgium

[2] Leibniz Institute for Analytical Sciences ISAS, e.V., Otto-Hahn-Str. 6b, 44227 Dortmund, Germany

[#] These authors contributed equally

CONTENT **page**

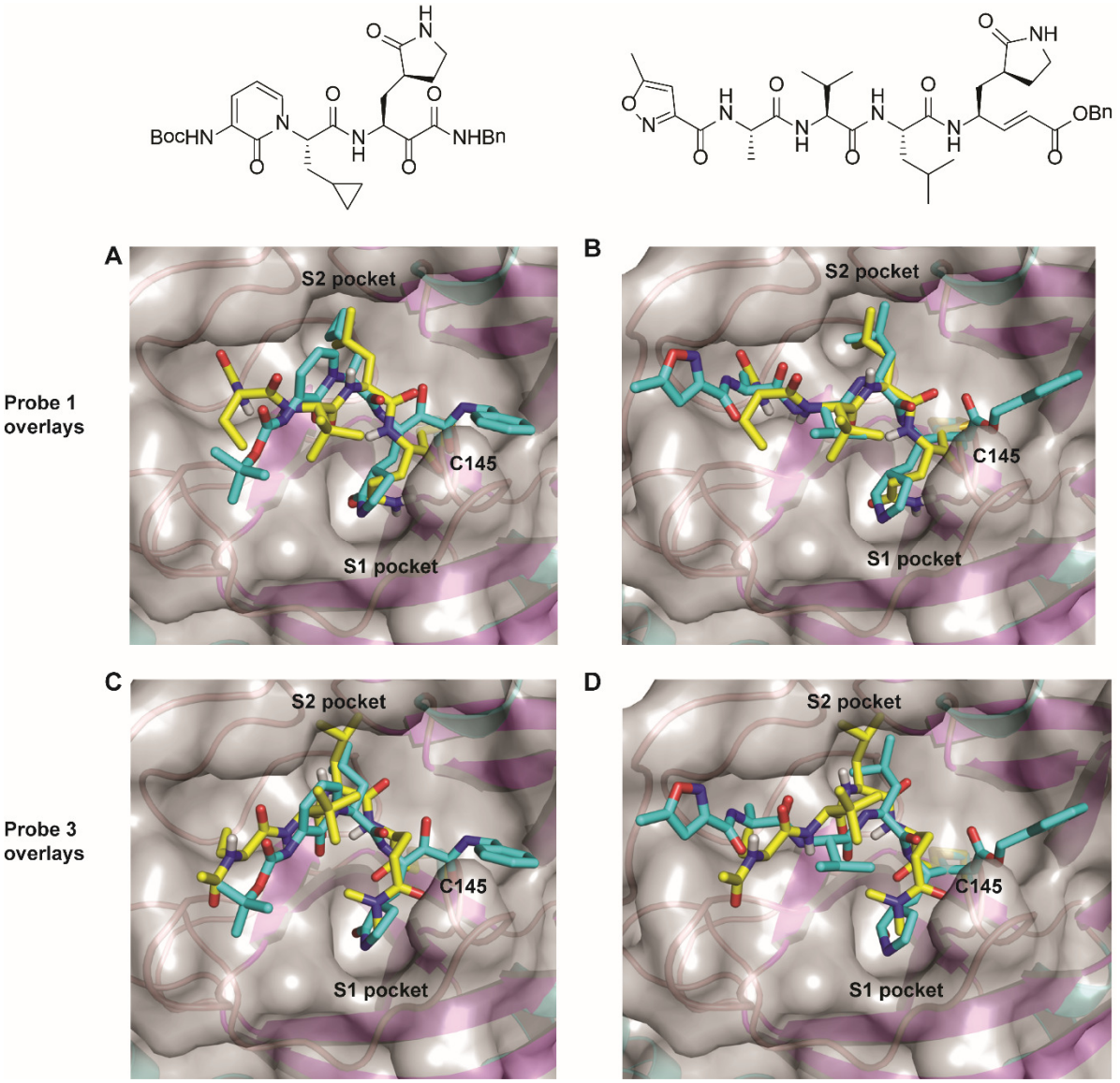

Figure S1. Close-up of the SARS-CoV-2 M^{pro} (PDB code: 6LZE) with docked probe **4** (panel A and B) and docked probe **6** (panel C and D), overlayed with the crystal structure of peptidyl ketoamide inhibitor from Zhang et al.[1] (panel A and C) or peptidyl vinyl benzyl ester from Jin et al.[2] (panel B and D). Protein is depicted as cartoons and a transparent surface (with β-sheets in magenta, helices in cyan and random coil in pink). The covalently bound inhibitors and the side chain of the active site C145 are drawn as sticks. Docked inhibitor in yellow and crystallized inhibitor in cyan. Pictures rendered in PyMol.[3]

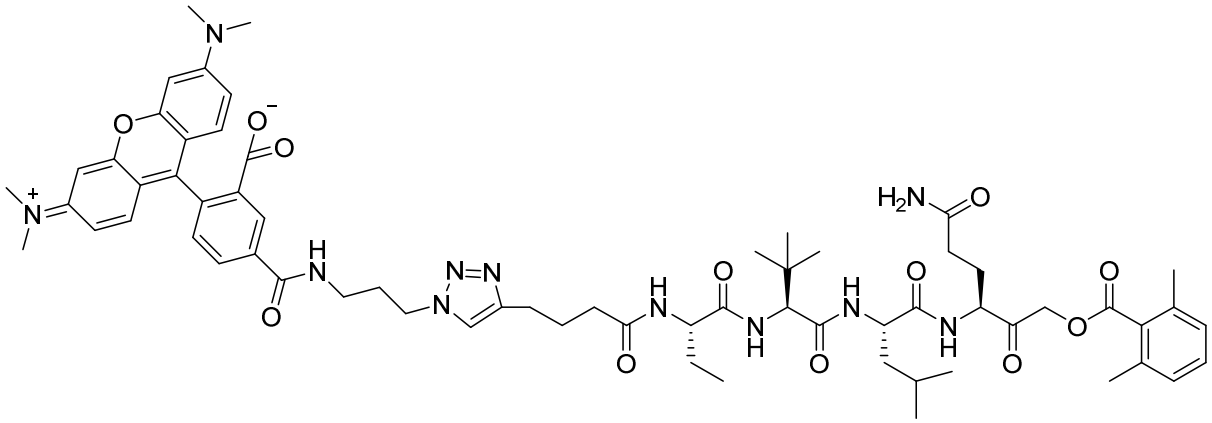

Figure S2. Full structure of pre-clicked probe **9**

General methods and materials

General chemistry

All starting materials and solvents were bought from commercial vendors and used without further purification. Reactions were analyzed by Thin Layer Chromatography (TLC) on pre coated 0.20 mm thick ALUGRAM® TLC sheets with fluorescent indicator and by liquid chromatography-mass spectrometry (LC-MS) performed on a Prominence Ultra-fast Liquid Chromatography system (Shimadzu) equipped with a 2x150 mm C18 analytical column (Waters X-Bridge) coupled to a MS-2020 single quadrupole mass analyzer (Shimadzu). Silica column chromatography was performed using 230-400 mesh silica (Kieselgel 60). High Pressure Liquid Chromatography (HPLC) purification was performed using a 10x150 mm C18 preparative column (X-Bridge). A linear gradient of 20-80% acetonitrile in water (with 0.1% TFA) was utilized. The purity of all final compounds tested was determined to be ≥95% using liquid chromatography-mass spectrometry (LC-MS).

Fmoc-Gln(Me)$_2$-tBu

Fmoc-L-glutamic acid 5-*tert*-butyl ester (Fmoc-Glu-tBu) was dissolved in DMF. 3 eq of benzotriazol-1-yl-oxytripyrrolidinophosphonium hexafluorophosphate (PyBoP), Di-isopropylethylamine (DIEA) and dimethylamine hydrochloride were added and reaction mixture was stirred for 3 hours at room temperature. The solvent was removed under pressure and the product was purified using column chromatography (PE:EA 4:1 to 1:1) to obtain a light yellow solid. (84% yield).

^{1}H NMR (400 MHz, $CDCl_3$) δ 7.79 (d, *J* = 7.5 Hz, 2H), 7.63 (t, *J* = 7.2 Hz, 2H), 7.42 (t, *J* = 7.5 Hz, 2H), 7.33 (td, *J* = 7.5, 1.1 Hz, 2H), 5.76 (d, *J* = 7.3 Hz, 1H), 4.45 – 4.32 (m, 2H), 4.32 – 4.22 (m, 2H), 3.00 (d, *J* = 10.6 Hz, 6H), 2.56 – 2.36 (m, 2H), 2.30 – 1.98 (m, 2H), 1.50 (s, 9H).

^{13}C NMR (101 MHz, $CDCl_3$) δ 172.90 (s), 171.16 (s), 156.25 (s), 143.97 (s), 143.75 (s), 141.31 (s), 127.73 (s), 127.09 (s), 125.18 (d, *J* = 8.1 Hz), 119.99 (s), 82.47 (s), 67.10 (s), 54.27 (s),

47.15 (s), 37.46 (s), 35.89 (s), 29.40 (s), 27.93 (d, *J* = 7.5 Hz). ESI-MS: m/z calculated for $C_{26}H_{32}N_2O_5$ [M+H] 453.23 found 452.95.

Fmoc-Gln(Me)$_2$-OH (2c)

tert-Butyl N2-(((9H-fluoren-9-yl)methoxy)carbonyl)-N5,N5-dimethylglutaminate (Fmoc-Gln(Me)$_2$-tBu) was dissolved in TFA:H_2O:TIPS (95:2.5:2.5) and stirred at room temperature for 1 hour. The solvent was removed under pressure and the product was used as crude for the next reaction. ESI-MS: m/z calculated for $C_{22}H_{24}N_2O_5$ [M+H] 397.17 found 396.95.

General synthesis of chloromethylketone derivatives

All amino acids were converted into chloromethyl ketones (CMKs) using a previously described synthetic procedure.[4] All CMK derivatives were obtained as yellow solids and used as crude in the next reaction.

Fmoc-Glu(tBu)-CMK (3a)

Crude yield: quant. ^{1}H NMR (400 MHz, $CDCl_3$) δ 7.78 (d, *J* = 7.5 Hz, 2H), 7.61 (dd, *J* = 7.0, 4.2 Hz, 2H), 7.38 (dtd, *J* = 34.7, 7.5, 0.8 Hz, 4H), 5.71 (d, *J* = 7.6 Hz, 1H), 4.59 (tt, *J* = 17.8, 8.9 Hz, 1H), 4.46 (ddd, *J* = 29.4, 10.6, 6.9 Hz, 2H), 4.34 – 4.25 (m, 2H), 2.44 – 2.11 (m, 3H), 1.91 (td, *J* = 14.9, 6.9 Hz, 1H), 1.47 (s, 9H). ^{13}C NMR (101 MHz, $CDCl_3$) δ 200.99 (s), 172.21 (s), 156.10 (s), 143.66 (d, *J* = 3.5 Hz), 141.36 (s), 127.82 (s), 127.12 (s), 125.03 (d, *J* = 7.4 Hz), 120.05 (s), 81.24 (s), 66.99 (s), 57.30 (s), 47.23 (s), 46.53 (s), 30.93 (s), 28.07 (s), 26.11 (s). ESI-MS: m/z calculated for $C_{25}H_{28}ClNO_5$ [M+H] 458.17 found 457.95.

Fmoc-Cit-CMK (3b)

Crude yield: quant. ^{1}H NMR (400 MHz, DMSO) δ 7.90 (d, *J* = 7.5 Hz, 2H), 7.81 (d, *J* = 7.7 Hz, 1H), 7.71 (d, *J* = 7.4 Hz, 2H), 7.43 (t, *J* = 7.4 Hz, 2H), 7.34 (dd, *J* = 10.7, 4.2 Hz, 2H), 5.95 (s, 1H), 5.39 (s, 2H), 4.58 – 4.47 (m, 2H), 4.38 (ddd, *J* = 22.6, 10.6, 6.8 Hz, 2H), 4.24 (t, *J* = 6.6 Hz, 1H), 4.17 (td, *J* = 9.4, 4.5 Hz, 1H), 2.94 (dd, *J* = 10.4, 5.6 Hz, 2H), 1.70 (d, *J* = 6.5 Hz, 1H),

1.52 – 1.21 (m, 3H). ^{13}C NMR (101 MHz, DMSO) δ 201.87 (s), 159.22 (s), 156.65 (s), 144.22 (s), 141.25 (s), 128.12 (s), 127.53 (s), 125.65 (d , *J* = 7.1 Hz), 120.60 (s), 65.98 (s), 58.45 (s), 48.09 (s), 47.24 (s), 27.24 (s), 26.97 (s). ESI-MS: m/z calculated for $C_{22}H_{24}ClN_3O_4$ [M+H] 430.15 found 429.90.

Fmoc-Gln(Me)$_2$-CMK (3c)

Crude yield: 77%. ^{1}H NMR (400 MHz, $CDCl_3$) δ 7.79 (d, *J* = 7.5 Hz, 2H), 7.62 (t, *J* = 7.0 Hz, 2H), 7.43 (t, *J* = 7.4 Hz, 2H), 7.34 (tdd, *J* = 7.4, 2.4, 1.1 Hz, 2H), 7.28 (s, 1H), 6.35 (s, 1H), 4.52 (ddd, *J* = 21.0, 17.7, 15.6 Hz, 2H), 4.43 – 4.30 (m, 2H), 4.23 (t, *J* = 7.0 Hz, 1H), 2.98 (d, *J* = 11.8 Hz, 6H), 2.58 – 2.32 (m, 2H), 2.29 – 1.99 (m, 2H). ^{13}C NMR (101 MHz, $CDCl_3$) δ 201.43 (s), 172.04 (s), 156.39 (s), 143.72 (d, *J* = 8.5 Hz), 141.35 (s), 127.79 (s), 127.09 (d, *J* = 4.6 Hz), 125.11 (d, *J* = 12.9 Hz), 120.04 (s), 67.01 (s), 58.07 (s), 47.21 (s), 46.77 (s), 37.22 (s), 35.68 (s), 28.90 (s), 26.03 (s). ESI-MS: m/z calculated for $C_{23}H_{25}ClN_2O_4$ [M+H] 429.15 found 428.90.

Fmoc-His(Boc)-CMK (3d)

Crude yield: 82%. ^{1}H NMR (400 MHz, $CDCl_3$) δ 8.04 (s, 1H), 8.01 (s, 2H), 7.79 (dd, *J* = 7.5, 3.9 Hz, 2H), 7.63 (dd, *J* = 14.4, 7.1 Hz, 2H), 7.46 – 7.39 (m, 2H), 7.38 – 7.31 (m, 2H), 7.18 (s, 1H), 6.27 (dd, *J* = 59.3, 7.8 Hz, 1H), 4.74 (ddd, *J* = 18.7, 12.9, 5.3 Hz, 1H), 4.54 – 4.16 (m, 5H), 3.14 (dtd, *J* = 20.2, 15.1, 5.2 Hz, 2H), 1.62 (d, *J* = 1.4 Hz, 9H). ^{13}C NMR (101 MHz, $CDCl_3$) δ 201.05 (s), 156.25 (s), 146.78 (s), 144.00 (s), 143.81 (s), 143.65 (s), 141.36 (s), 137.91 (s), 136.94 (s), 127.74 (d, *J* = 13.5 Hz), 127.07 (s), 125.15 (s), 120.00 (d, *J* = 9.6 Hz), 115.06 (s), 85.94 (s), 67.07 (s), 61.50 (s), 57.91 (s), 53.75 (s), 47.28 (d, *J* = 7.7 Hz), 30.15 (s), 29.05 (s), 27.88 (s), 14.18 (s). ESI-MS: m/z calculated for $C_{27}H_{28}ClN_3O_5$ [M+H] 510.17 found 509.95.

Fmoc-Glu(tBu)-AOMK

Fmoc-Glu(tBu)-CMK was dissolved in DMF and 2,6 dimethyl benzoic acid (1.5 eq) and potassium fluoride (3 eq) were added. Reaction mixture was stirred overnight at room

temperature. The solvent was removed under pressure and the reaction mixture was dissolved in ethyl acetate and washed with 3x brine solution and 3x saturated aqueous NaHCO3 solution. The resulting product was purified using column chromatography (PE:EA 4:1 to 1:1) to obtain a light yellow solid (73% yield). ^{1}H NMR (400 MHz, $CDCl_3$) δ 7.79 (d, *J* = 7.5 Hz, 2H), 7.63 (dd, *J* = 7.2, 4.1 Hz, 2H), 7.43 (t, *J* = 7.4 Hz, 2H), 7.34 (td, *J* = 7.4, 1.0 Hz, 2H), 7.26 – 7.20 (m, 1H), 7.06 (dd, *J* = 14.6, 7.5 Hz, 2H), 5.70 (d, *J* = 7.5 Hz, 1H), 5.08 (dd, *J* = 43.3, 16.9 Hz, 2H), 4.59 – 4.38 (m, 3H), 4.24 (t, *J* = 6.8 Hz, 1H), 2.43 (s, 6H), 2.32 (ddd, *J* = 24.5, 11.3, 6.3 Hz, 3H), 1.97 (td, *J* = 14.4, 6.5 Hz, 1H), 1.48 (s, 9H). ^{13}C NMR (101 MHz, $CDCl_3$) δ 201.88 (s), 172.33 (s), 169.02 (s), 156.15 (s), 143.67 (s), 141.36 (s), 135.71 (s), 132.42 (s), 129.75 (s), 127.74 (d, *J* = 8.0 Hz), 127.12 (s), 125.04 (s), 120.03 (s), 81.18 (s), 67.09 (s), 66.61 (s), 56.97 (s), 47.22 (s), 30.96 (s), 28.08 (s), 26.36 (s), 19.90 (s). ESI-MS: m/z calculated for $C_{34}H_{37}ClNO_7$ [M+H] 572.26 found 572.10.

Loading of chloromethyl ketone derivatives and synthesis of 2,6-dimethylbenzoyloxymethyl ketone derivatives on hydrazine resin

A 0.5 M solution of 3 eq Fmoc-AA-CMK was added to the resin in a solid phase cartridge and gently shaken at 50 ºC for 3 hours. After incubation, the solution was removed and resin was washed 3 times with DMF. 5 eq of 2,6-dimethylbenzoic acid and 10 eq potassium fluoride in DMF were added and the reaction mixture was gently shaken overnight at room temperature. The solution was removed and the resin was washed 3 times with methanol, DMF and DCM, and dried. The resin loading was estimated by UV absorption of free Fmoc at 290 nm. Standard SPPS protocol was used for the rest of the synthesis.

Loading of acyloxymethylketone derivatives on RINK resin

Fmoc-Glu(tBu)-AOMK was dissolved in TFA:H_2O:Triisopropyl silane(TIPS) (95:2.5:2.5) and stirred at room temperature for 1 hour. The solvent was removed under pressure and the product was used as crude for the next reaction. Rink resin was swollen in DMF for 5 minutes. The Fmoc protecting group was removed using 20% piperidine in DMF. A 0.2 M solution of

Fmoc-Glu-AOMK in DMF was added to the resin in a solid phase cartridge, together with 3 eq of HOBt/DIC. The reaction was gently shaken at room temperature for 3 hours. After incubation, the solution was removed and resin was washed 3 times with DMF and DCM. The resin loading was estimated by UV absorption of free Fmoc at 290 nm. Standard SPPS protocol was used for the further synthesis.

General SPPS protocol

The N-terminal Fmoc group was removed by incubating the resin with 5% diethylamine (DEA) in DMF for 2 times 15 min. The resin was washed 3 times with DMF and DCM. 3 eq *N*-Fmoc-protected amino acid and 3 eq of HOBt/DIC were dissolved in DMF (0.2 M final concentration) and added to the resin. The resin was shaken at room temperature for 3 hours, and washed 3 times with DMF and DCM. For each subsequent step of the solid phase peptide synthesis, the same deprotection and coupling reactions were used. However, when an amino acid was coupled to the free amine group of t-butyl-glycine (Tle), the Fmoc amino acid (3 eq) was preactivated with 3 eq of HATU/DIPEA for 2 min, added to the resin and gently shaken for 3h at room temperature. Coupling reactions were monitored by Kaiser test. All probes were capped with 5-Hexynoic acid, which was coupled using 3 eq DIC/HOBt in DMF. The final product was cleaved off the resin with a TFA/TIPS/H_2O mixture (v/v/v, 95:2.5:2.5) and the solvent was removed under pressure. The final product was purified by reversed-phase HPLC. Fractions containing product were pooled and lyophilized.

Probe 4. 1.3% yield. ESI-MS: m/z calculated for $C_{37}H_{55}N_5O_8$ [M+H] 698.41 found 698.25.

Probe 5. 3.5% yield. ESI -MS: m/z calculated for $C_{38}H_{58}N_6O_8$ [M+H] 727.43 found 727.25.

Probe 6. 2.1% yield. ESI -MS: m/z calculated for $C_{39}H_{59}N_5O_8$ [M+H] 726.44 found 726.25.

Probe 7. 6.7% yield. ESI -MS: m/z calculated for $C_{31}H_{48}N_6O_7$ [M+H] 617.36 found 617.20.

Probe 8. 5.2% yield. ESI -MS: m/z calculated for $C_{29}H_{46}N_6O_6$ [M+H] 575.35 found 575.15.

Synthesis of probe 9

Probe **4** was dissolved in DCM and 1 eq of CuBr and 3 eq of DIPEA were added. Lastly, 1.05 eq of 5-Carboxytetramethylrhodamine Azide (5-TAMRA-Azide) was added. Reaction mixture was stirred for 1 hour at room temperature. The solvent was removed under pressure and the final probe was purified by reversed-phase HPLC. Fractions containing product were pooled and lyophilized. Probe **9** was obtained as a red powder in 23.7% yield.

ESI -MS: m/z calculated for $C_{65}H_{83}N_{11}O_{12}$ [M+H] 1211.62 found 1211.45.

Recombinant expression of SARS-CoV-2 in E. Coli and purification

The expression and purification of M^{pro} was performed following the protocol reported by Zhang et al.,[1] with some modifications. In short, a freshly transformed E. Coli BL21 single colony containing the SARS-CoV-2 Mpro construct in a PGEX-6p-1 vector, was inoculated in LB supplemented with ampicillin (100 ug/mL) and grown for 3 hours at 37 ºC. This LB was then diluted 80 times into LB supplemented with ampicillin (100 ug/mL) and incubated at 37ºC until the OD600 was 0.7 - 0.8 when the expression was induced by addition of 0.5 mM IPTG. The induced cultures were left at 16 º C for 8 hours. After that time the cells were harvested by centrigugation at 5500 rpm at 4 ºC for 15 min. The pellets were resuspended in 30 mL buffer A (20 mM Tris, 150 mM NaCl, pH 7.8; pH of all buffers was adjusted at room temperature) and then lysed by sonication on ice, 10 cycles of 10s on 30 s off or using a high pressure emulsifier. The cellular membranes were removed by ultracentrifugation at 145,000 x g at 4°C for 1 h. The supernatant was subjected to nickel-nitrilotriacetic acid beads (Qiagen; 1 mL beads per 1 L bacterial expression culture) for 1 hour at 4ºC and eluted by increasing imidazole washing steps (25 mM, 50 mM, 200 mM, and 500 mM final elution in 20 mM Tris, 150 mM NaCl, pH 7.8. The protein concentration of the Mpro containing fractions (those at 200 mM Imidazole) was assessed and then diluted with buffer A to a final concentration of 1mg/mL in order to avoid protein precipitation. Then PreScission protease was added to cleave the 6xHis-tag, following the instructions of the commercial vendor (Sigma Aldrich, ref GE27-0843-01). The protease mixture was transferred into a dialysis cassette 10K cutoff and dialyzed against

reaction buffer 1 (20 mM Tris, 150 mM NaCl, 1 mM DTT, 1mM EDTA, pH 7.8) or reaction buffer 2 (20 mM HEPES-NaOH, 150 mM NaCl, 1 mM DTT, pH 7.8) at 4ºC for 22 hours, to ensure the cleavage completion. In order to remove the PreScission protease, the solution containing Mpro with the authentic N- and C termini was incubated with GST-beads for 1 hour at room temperature. After this time the whole was span down using a tabletop centrifuge at 500 g, 4ºC, 10 min and the supernatant collected. Two washes with either reaction buffer 1 or reaction buffer 2. The combined fractions were then concentrated to a third of their volume using an Amicon Ultra 15 centrifugal filters (10 kD,Merck Millipore) at 3000 rpm, and 4ºC.

Inhibition assay

Purified M^{pro} was diluted in reaction buffer (50 mM Tris, 150 mM NaCl, 1 mM EDTA and 1 mM DTT, pH 7,1) to a concentration of 200 nM and added in each well of a black, flat-bottom, 96-well microplate in a total volume of 100 µL per well. 1 µL of inhibitor in DMSO was added to the desired final concentration and incubated for 1 hour at 37 °C, followed by the addition of 1 µL of Ac-Abu-Tle-Leu-Gln-MCA substrate in DMSO (Peptides International) at a final concentration of 200 µM. Fluorescence was measured and fluorescence was measured for 15 minutes at 355 nm excitation and 460 nm emission in a SpectraMax iD3 Multi-Mode Microplate Reader (Molecular Devices) at 37 °C. All experiments were performed in triplicate. For quantification, linear segments of cleavage activity were taken and normalized against the DMSO treated controls.

Covalent docking

Probe **4-8** were attached to the side chain of residue CYS145 of chain A of (PDB: 6lze) and docked according to the flexible side chain method. The probes input file was drawn in Chemdraw professional 15.1, converted to a pdb file using Chem3D 15.1 and converted into a PDBQT by autodocktools 1.5.6. The connected complex was treated as a fully flexible side chain. The binding site was covered by preparing a 42x50x48 size grid box with grid spacing of 0.375 Å and the center at -10.22, 13.388, 67.854.

Preparation of E. Coli uninduced lysates

Escherichia coli strain BL21 (DE3) was grown in 500 mL LB at 37ºC and 300 rpm for 16 hours. After this time the cells were pelleted at 5000 rpm at 4ºC for 30 min. Pelleted cells were lysed by sonication on ice (10 passages 10 sec on 30 sec off) in lysis buffer (20 mM Tris, 150 mM NaCl, pH 7.8). The lysate was ultracentrifuged at 146,682 x *g* at 4°C for 1 h.and aliquoted. A part of the aliquoted lysate was subjected to dialysis against 20 mM HEPES-NaOH, 150 mM NaCl, 1 mM DTT, pH 7.8 overnight at 4ºC.

Labeling purified M^{Pro}

220 ng of purified M^{pro} was diluted in 30 µL HEPES buffer (50 mM HEPES, 150 mM NaCl, 1 mM DTT, pH 7.5) and incubated with 5, 1 or 0.2 µM probe **1** or **3** for 1 h at 37 °C. After incubation with the probes, 25 µM TAMRA-azide or 25 µM biotin-azide, 50 µM THPTA, 500 µM $CuSO_4$ (stock was prepared fresh before use) and 500 µM sodium ascorbate (stock was prepared fresh before use) were added to each sample. Samples were incubated at room temperature for 1 hour. After incubation, the samples were mixed with 4x SDS-loading buffer and boiled at 95 °C for 5 min. After separation of half of the sample (110 ng) by 15% SDS-PAGE, the TAMRA gel was scanned on a Typhoon FLA 9500. The biotin clicked probe proteases were visualized by Western Blot by transferring to nitrocellulose, blocking with 3% milk, washing with PBST (3 x 5 min), incubation with streptavidin-HRP (Sigma Aldrich; 1:3500 dilution of a 1 mg/mL stock) for 1h, washing with PBST (3 x 15 min) and detection by home made ECL.

Labeling in bacterial lysates

Both induced and non-induced lysates were diluted to a total protein concentration of 500 µg/mL with HEPES buffer (50 mM HEPES, 150 mM NaCl, 1 mM DTT, pH 7.5). Some samples were preincubated with 50 µM carmofur for 1 hour at 37 °C. After incubation, each sample was incubated with 5 µM of either probe **1, 3** or **6** for 1 hour at 37 °C. After incubation with the

probes, 25 µM TAMRA-azide, 50 µM THPTA, 500 µM $CuSO_4$ (stock was prepared fresh before use) and 500 µM sodium ascorbate (stock was prepared fresh before use) were added to each sample, except the samples that were treated with pre-clicked probe **6**. Samples were incubated with the click reagents at room temperature for 1 hour. After incubation, the samples were mixed with 4x SDS-loading buffer and boiled at 95 °C for 5 min. After separation by 15% SDS-PAGE, the gel was scanned on a Typhoon FLA 9500.

Preparation HEK 293T lysates

HEK293T cells were grown in DMEM media (D6546-500ML Sigma) supplemented with 10% FBS, 2 mM glutamax, 100 units/ml penicillin, and 0.1 mg/ml streptomycin. They were maintained at 37 °C with 5% CO2. Cells were split every 3 to 4 days according to ATCC protocol. For making lysates, cells were harvested and collected by centrifugation (400 g for 5 min at 4 °C). Supernatant was removed and the amount (approx. volume) of pellets was estimated. The pellets were washed twice with ice-cold PBS and resuspended in 5 vol of ice-cold buffer A (20 mM HEPES, 10 mM KCl, 2 mM EDTA, 1 mM DTT) supplemented with protease inhibitors. After sitting on ice for 15 min, the cells were broken by passing 15 times through a G25 needle. After centrifugation in a microcentrifuge for 15 min at 4 °C, the supernatants were further centrifuged at 17×10^3 g for 15 min at 4 °C and flash frozen in liquid N_2 for use as lysates, with a total protein concentration of 3 mg/mL.

Labeling in HEK 293T lysates

HEK 293T lysates were spiked with different quantities of purified M^{pro} and incubated with 5 µM of probe **6** for 1 hour at 37 °C. After incubation, the samples were mixed with 4x SDS-loading buffer and boiled at 95 °C for 5 min. After separation by 15% SDS-PAGE, the gel was scanned on a Typhoon FLA 9500.

Copies of chromatograms

Probe **4**

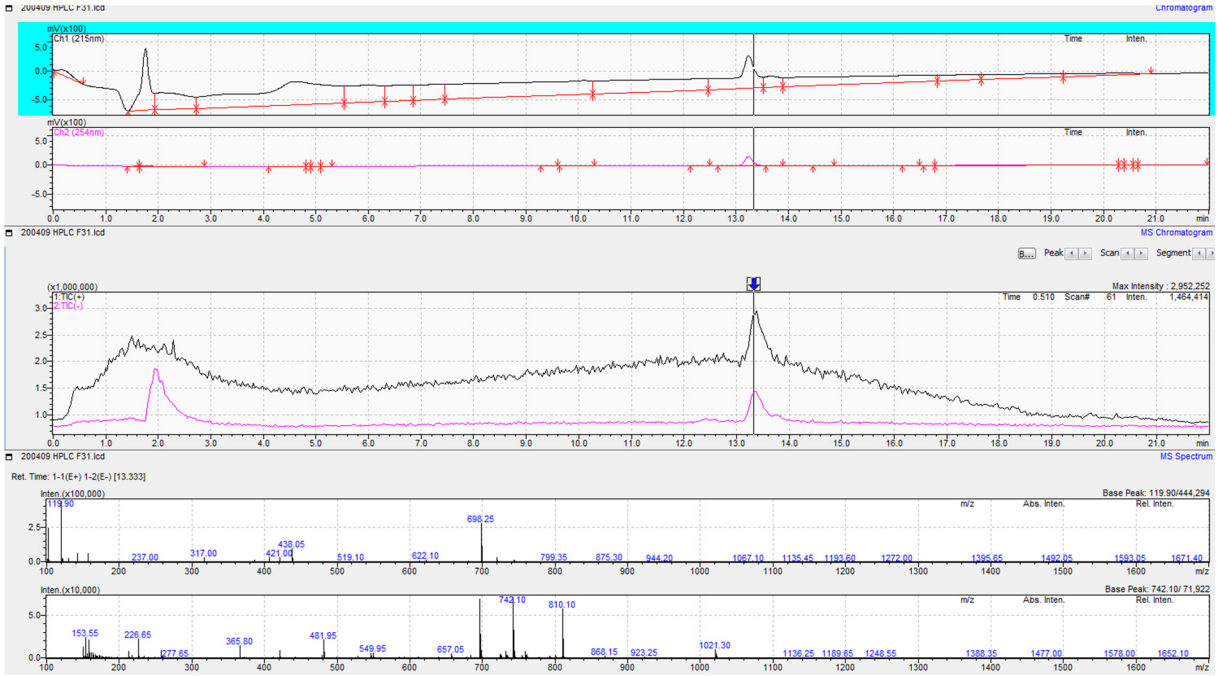

Probe **5**

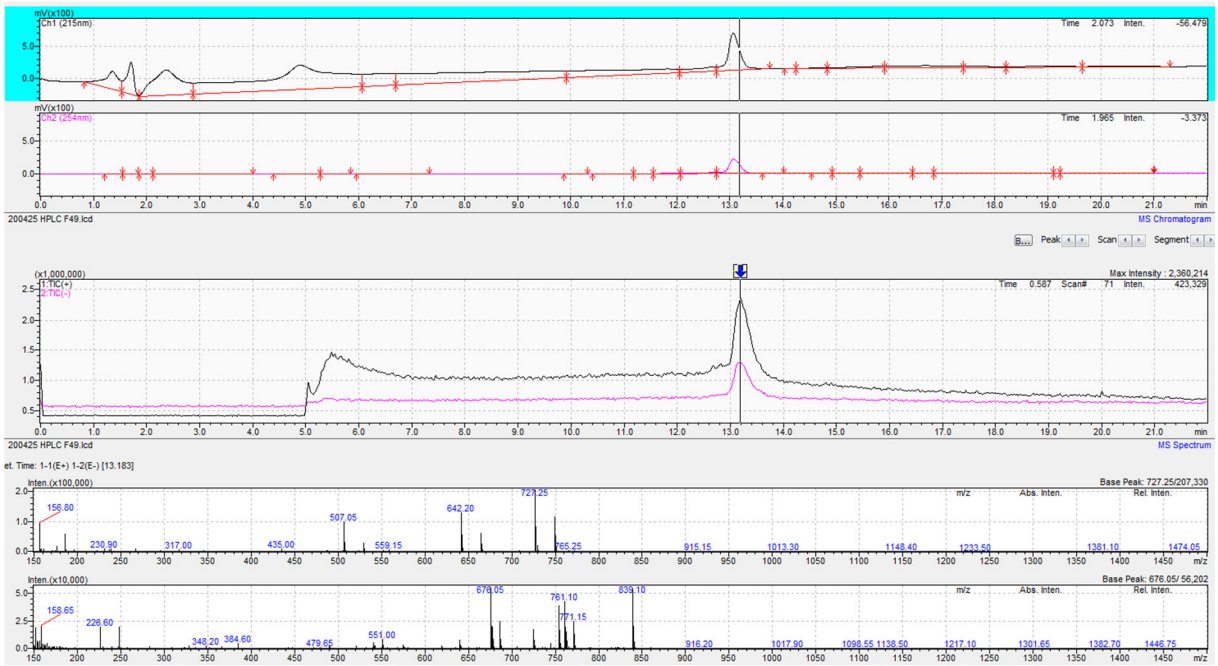

Probe **6**

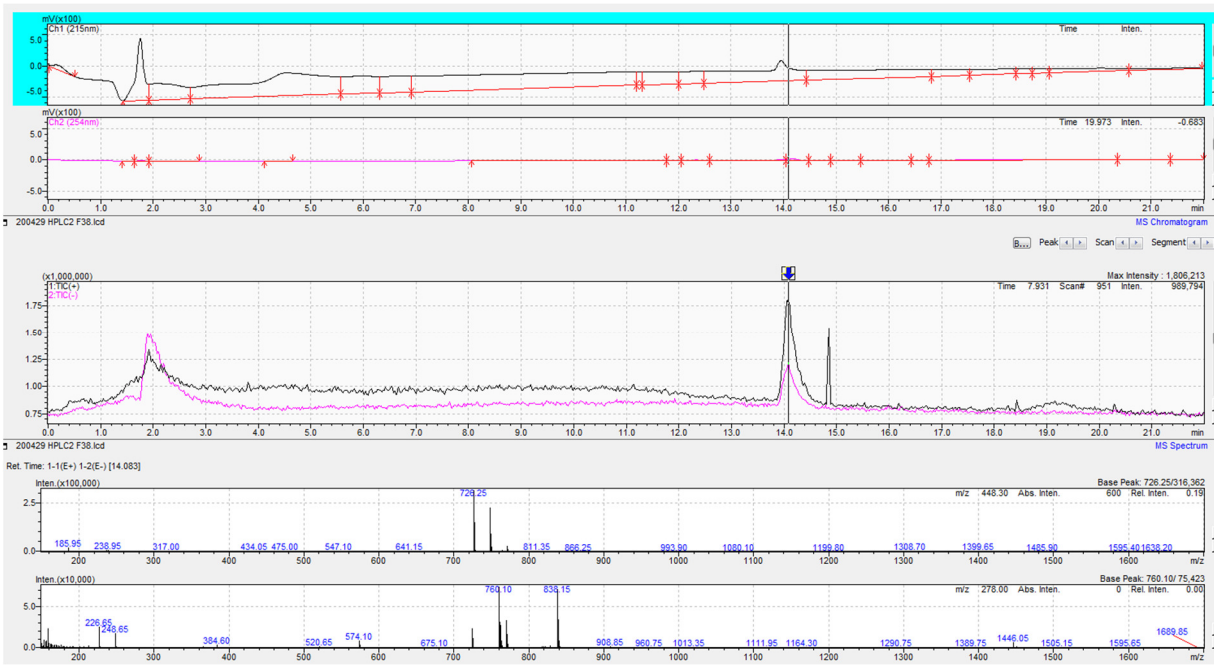

Probe **7**

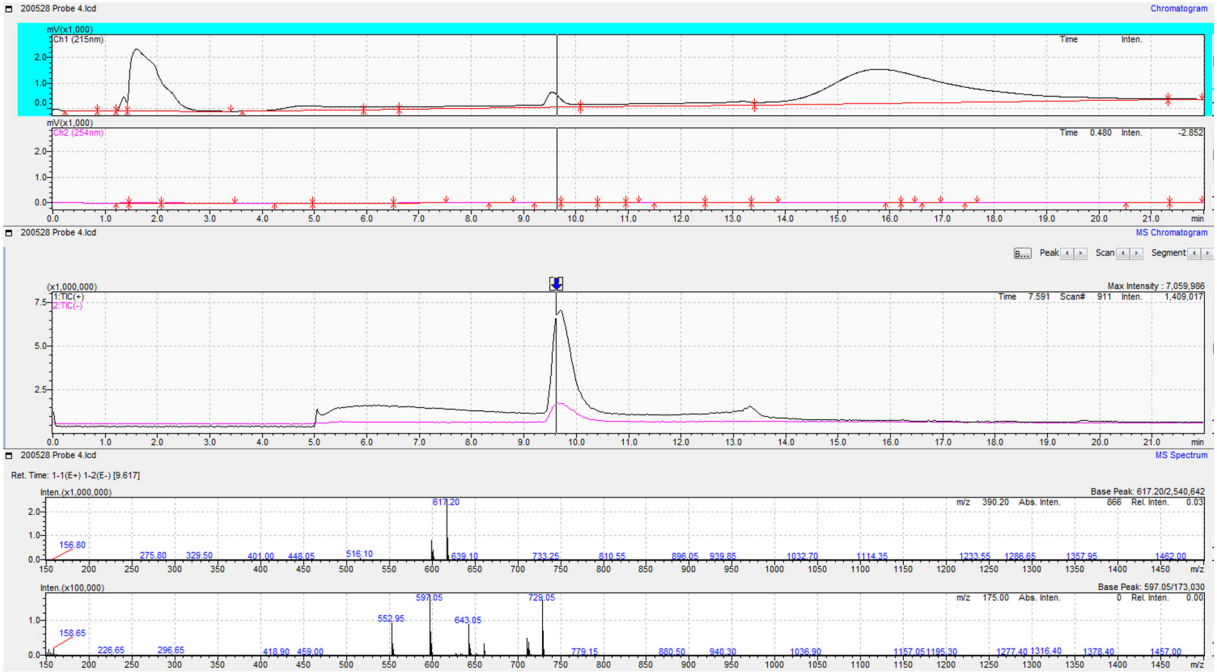

Probe **8**

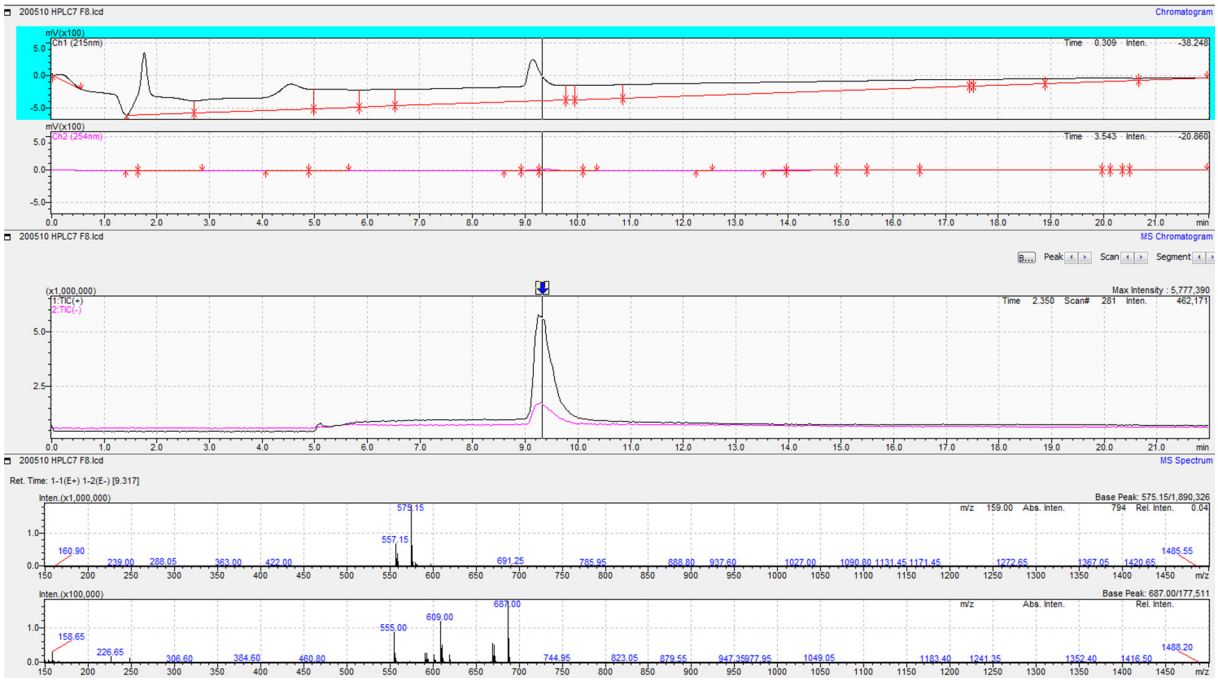

Probe **9**

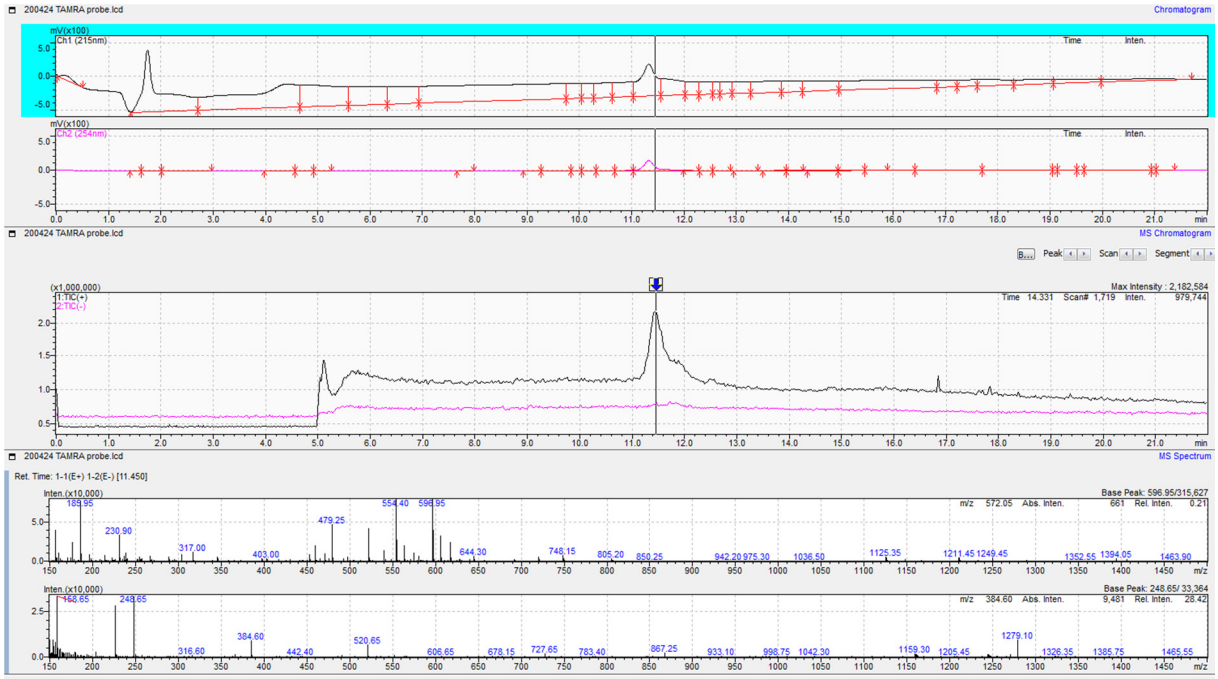

Supplemental references

1. Zhang, L., Lin, D., Sun, X., Curth, U., Drosten, C., Sauerhering, L., Becker, S., Rox, K., and Hilgenfeld, R. (2020) Crystal structure of SARS-CoV-2 main protease provides a basis for design of improved alpha-ketoamide inhibitors, *Science 368*, 409-412.
2. Jin, Z., Du, X., Xu, Y., Deng, Y., Liu, M., Zhao, Y., Zhang, B., Li, X., Zhang, L., Peng, C., Duan, Y., Yu, J., Wang, L., Yang, K., Liu, F., Jiang, R., Yang, X., You, T., Liu, X., Yang, X., Bai, F., Liu, H., Liu, X., Guddat, L. W., Xu, W., Xiao, G., Qin, C., Shi, Z., Jiang, H., Rao, Z., and Yang, H. (2020) Structure of M(pro) from SARS-CoV-2 and discovery of its inhibitors, *Nature*.
3. Delano, W. L. (2002) The Pymol Molecular Graphics Systems (http://www.pymol.org).
4. Kato, D., Boatright, K. M., Berger, A. B., Nazif, T., Blum, G., Ryan, C., Chehade, K. A. H., Salvesen, G. S., and Bogyo, M. (2005) Activity-based probes that target diverse cysteine protease families, *Nat. Chem. Biol. 1*, 33-38.

Peptidyl Acyloxymethyl Ketones as Activity-Based Probes for the Main Protease of SARS-CoV-2

Merel A. T. van de Plassche,[1#] Marta Barniol-Xicota,[1#] and Steven H. L. Verhelst[*, 1,2]

[1] KU Leuven, Department of Cellular and Molecular Medicine, Laboratory of Chemical Biology, Herestr. 49, 3000 Leuven, Belgium

[2] Leibniz Institute for Analytical Sciences ISAS, e.V., Otto-Hahn-Str. 6b, 44227 Dortmund, Germany

[#] These authors contributed equally

* Corresponding author: steven.verhelst@isas.de, steven.verhelst@kuleuven.be

Abstract

The global pandemic caused by SARS-CoV-2 calls for a fast development of antiviral drugs against this particular coronavirus. Chemical tools to facilitate inhibitor discovery as well as detection of target engagement by hit or lead compounds from high throughput screens are therefore in urgent need. We here report novel, selective activity-based probes that enable detection of the SARS-CoV-2 main protease. The probes are based on acyloxymethyl ketone reactive electrophiles combined with a peptide sequence including non-natural amino acids that targets the non-primed site of the main protease substrate binding cleft. They are the first activity-based probes for the main protease of coronaviruses and display target labeling within in a human proteome without background. We expect that these reagents will be useful in the drug development pipeline, not only for the current SARS-CoV-2, but also for other coronaviruses.

Although coronaviruses that infect humans have been known since 1966,[1 2] they have gained more global attention since the turn of the millennium, with the appearance of several strains that caused more severe symptoms and were more widely spread. Two outbreaks in 2002 and 2012, which were caused by severe acute respiratory syndrome coronavirus (SARS-CoV)[3] and Middle-East respiratory syndrome coronavirus (MERS-CoV),[4] respectively, were contained regionally. In December 2019, a novel coronavirus, later termed SARS-CoV-2 appeared in the province of Wuhan, China,[5] which led to a global pandemic that is currently ongoing. The clinical manifestations range from asymptomatic to fever and severe pneumonia known as covid-19, which in some cases can lead to death.[6] The virus has caused a worldwide crisis in healthcare, economy and society, and has painfully exposed the vulnerability of modern civilization. Currently, there is an ongoing global effort to develop vaccines and drugs that can eradicate SARS-CoV-2 and contain the pandemic. Unfortunately, the immune response against the virus is not well understood, and it is unclear whether infected people build up immunity against reinfection. This emphasizes the importance for the development of drugs that inhibit coronavirus replication.

Coronaviruses - or coronaviridae - are enveloped, single stranded RNA viruses with a typical appearance of the solar corona caused by the viral spike protein that is part of the viral capsid. The replicase gene of the virus contains two overlapping open reading frames (ORFs) that are translated in two large polyproteins.[7] These polyproteins are proteolytically processed into 16 non-structural proteins (nsp1 to nsp16) by two viral proteases. Whereas the papain-like protease (PL^{pro}) performs three cuts to release nsp1-3, the main protease (M^{pro}, also called $3CL^{pro}$ for 3C-like protease) cuts at 11 sites, thereby liberating the most important protein products for replication.[7 8] Therefore, the M^{pro} has attracted major interest as a potential drug target.

M^{pro} is a protease from the C30 family.[9] Its active site comprises a catalytic dyad formed by a cysteine and histidine residue. The substrate specificity is governed by a requirement for Gln in the P1 position, and preferences for large hydrophobic residues in P2 and small residues in P1'.[10 11] Recently, the Drag laboratory has reported a substrate library screen incorporating a

large series of non-natural amino acids in a comparison of M^{pro} from SARS-CoV and SARS-CoV-2.[12] In the past, information on substrate specificity has been instrumental in the design of active site directed M^{pro} inhibitors - especially of peptidomimetics,[13] whereas crystallography has increased our structural understanding of the interactions between inhibitors and M^{pro} for further optimization.[14] Since the start of the 2019 SARS-CoV-2 pandemic, several crystal structures of the M^{pro} in complex with various inhibitors, such as peptidyl ketoamides, peptide aldehydes and peptidyl vinyl methyl esters, have been published.[15] [16] [17]

In the past, activity-based protein profiling (ABPP) has been particularly useful for the study of proteases.[18] [19] Activity-based protein profiling (ABPP) is a powerful technique to detect active enzymes in complex proteomes, such as cell lysates, whole cells or in vivo.[20] It relies on small molecules called activity-based probes (ABPs) that specifically form covalent bonds with active site residues of the target enzyme in a mechanism-based reaction. Although ABPP has been extensively applied for the characterization for the study of cancer-related enzymes[21] as well as enzymes from infectious bacteria,[22] application to viral infections has been much less investigated.[23] One of the underlying reasons may be the lack of ABPs specifically designed for viral targets, except for probes targeting the NS2B-NS3 protease of flaviviruses[24] [25] and the smallpox virus protease K7L.[26]

Here, we report the first ABPs for the Mpro of coronaviruses, exemplified by a probe for the Mpro of the recent SARS-CoV-2. It is based on a cysteine specific reactive electrophile and recent substrate specificity information combining natural and non-natural amino acids. We show that these probes detect the active form of the Mpro, are highly selective and can distinguish the protease within a human proteome.

Results and discussion

Probe design - As a warhead for the M^{pro} ABPs we chose the acyloxymethyl ketone (AOMK) reactive electrophile, because it is selective for cysteine proteases and compatible with solid phase peptide synthesis.[27] To guide this warhead towards the active site cysteine of the SARS-CoV-2 M^{pro}, we incorporated a peptide element matching the substrate specificity. Because

the glutamine side chain may react with the ketone moiety of the AOMK in a cyclization reaction, as reported before for glutaminyl fluoromethyl ketones,[28] we also incorporated a citrulline as possible glutamine mimic, a dimethylated Gln and a His, which both have been used as P1 residue in M^{pro} inhibitors.[13] For the P2-P4 position, we chose Abu-Tle-Leu, which is the recently reported optimal sequence for SARS-CoV-2 M^{pro}.[12] However, for the P1 His molecules, a Thr-Val-Cha sequence was selected, because this was reported to be a potent sequence for the biologically similar SARS 3CL Protease.[29] As a detection handle, we chose a hexynoic acid, since it allows for click chemistry-mediated introduction of various tags.

Probe synthesis - For the solid phase synthesis of the AOMK M^{pro} ABPs, we first synthesized the necessary chloromethyl ketone (CMK) building blocks of properly protected glutamine, dimethyl glutamine (made from commercially available building block **1**), citrulline and histidine, by activation of the carboxylic acid with isobutyl chloroformate, subsequent reaction with diazomethane and quenching with hydrochloric acid (Scheme 1A). The His CMK could not be made with the more standard trityl protecting group, not only because of the lability of the protecting group under acidic conditions, but also because of substitution of the chloride by the imidazole nitrogen in part of the product. Fortunately, with the more electron withdrawing Boc protecting group on the His side chain, CMK building block **3d** was obtained in a satisfactory crude yield of 82%.

For the construction of the probes, we took two different solid phase approaches. The probe with a P1 Gln side chain offered the opportunity to attach it by its side chain to a solid support. To this end, CMK building block **3a** was first converted into an AOMK by reaction with dimethylbenzoic acid, before removal of the *tert*-butyl protecting group and coupling to the Rink amide resin (Scheme 1B). Elongation with the appropriate Fmoc-protected amino acids, capping with a hexynoic acid and cleavage from resin yielded probe **4**. The compounds with a dimethyl Gln, Cit or His in the P1 position were made by loading the corresponding CMKs **3b-d** onto a semicarbazide resin, follwed by substitution with dimethylbenzoic acid, elongation and cleavage from the resin (Scheme 1C). Unfortunately, after cleavage from the resin and

concomitant cleavage of side chain protecting groups (where present), the compounds with a P1 His residue immediately hydrolyzed to hydroxymethyl ketones (HMKs) **7-8**, probably assisted by the imidazole side chain (Scheme 1D).

Scheme 1. synthesis of M^{pro} ABPs[a]

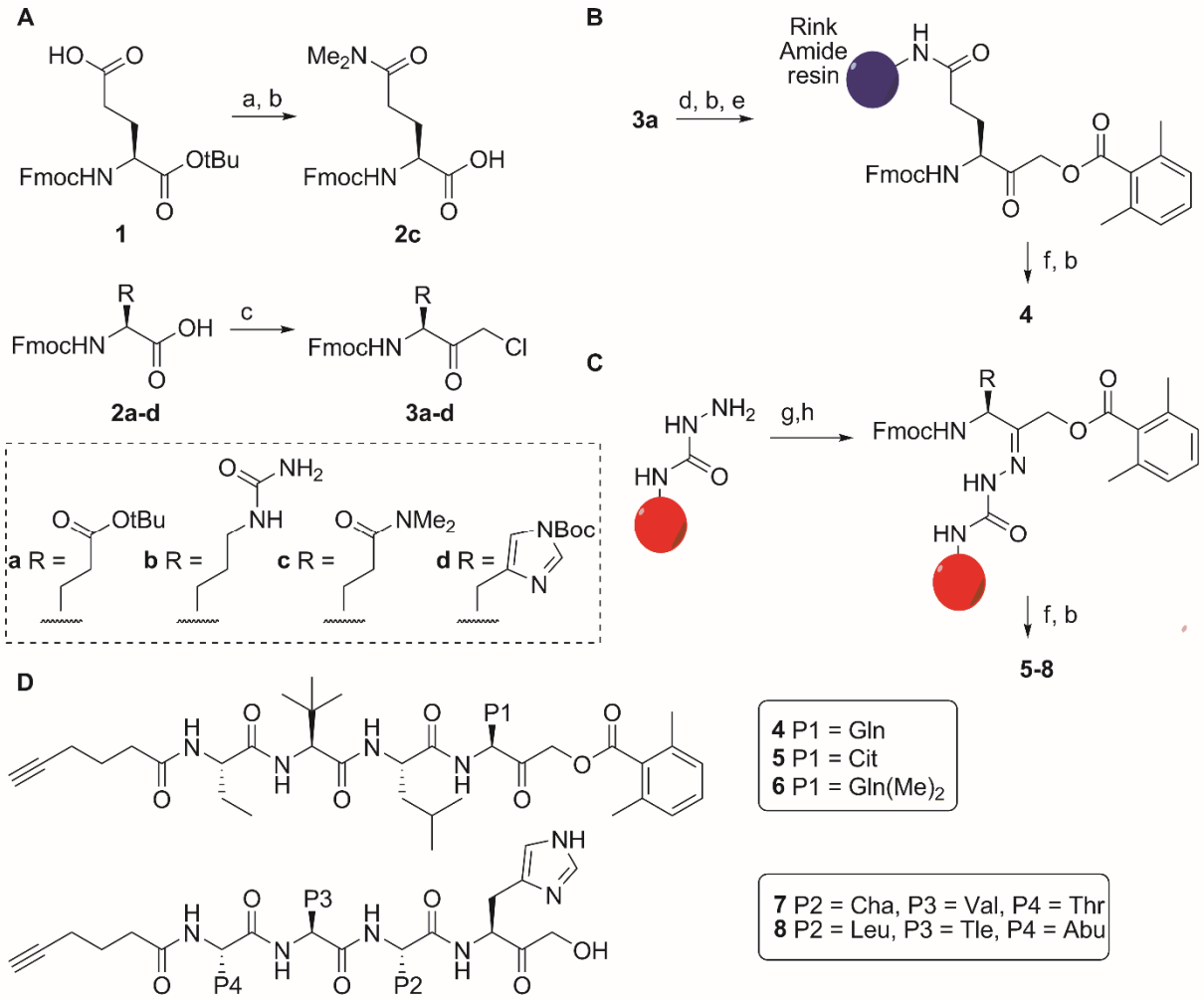

[a] Reagents and conditions: (a) dimethylamine hydrochloride, PyBoP, DIEA, DMF; (b) TFA/H_2O/triisopropylsilane (95/2.5/2.5); (c) 1. Isobutylchloroformate, N-methyl morpholine, THF; 2. Diazomethane, diethyl ether; 3. HCl (conc)/AcOH 1/1; (d) 2,6-dimethylbenzoic acid, KF, DMF; (e) Rink Amide Resin, diisopropyl carbodiimide, hydroxybenzotriazole, DMF; (f) Elongation by: 1. Fmoc deprotection using 5% diethylamine in DMF, 2. Fmoc-amino acid with

diisopropyl carbodiimide and hydroxybenzotriazole or HATU and diisopropylethylamine in DMF. (g) incubation with CMK **3b-d** in DMF at 50 ºC. (h) 2,6-dimethylbenzoic acid, KF, DMF.

Evaluation of inhibition – Compounds **4-8**, were evaluated an inhibition assay on purified SARS-CoV-2 M^{pro}, and compared to the recently reported M^{pro} active site inhibitor carmofur.[16 30] In short, the protease was incubated with the compound for 1 hour, after which a fluorogenic aminomethyl coumarin substrate[12] was added to measure residual activity. Compounds **4** and **6** showed clear inhibition of the protease, with probe **6** being most potent, but **5** and **8** did not show any activity (Figure 1A). Interestingly, probe **7** was still able to inhibit M^{pro} to some degree, even without its ability to form a covalent bond with the protease, illustrating that a His is still accepted in the P1 position.

To gain insight in the binding modes of the different probes, we performed covalent docking of the probe **4** - **8** in complex with Mpro using the flexible side chain method of Autodock 4.2.[31] The P1 and P2 amino acid residues of probe **4** and **6** both dock well into the corresponding S1 and S2 pockets of the enzyme (Figure 1C-E). Moreover, they display good overlap with crystal structures of various different peptidomimetic inhibitors (Figure 1D and Figure S1). However, probe **5** with Cit in the P1 position does not fit well into the active site (Figure 1F). Repeated runs of docking did not result in placement of the P1 Cit into the S1 pocket, likely due to its larger side in comparison with Gln, which explains the lack of potency of probe **5** and confirms the importance of the S1 pocket for inhibitor design.

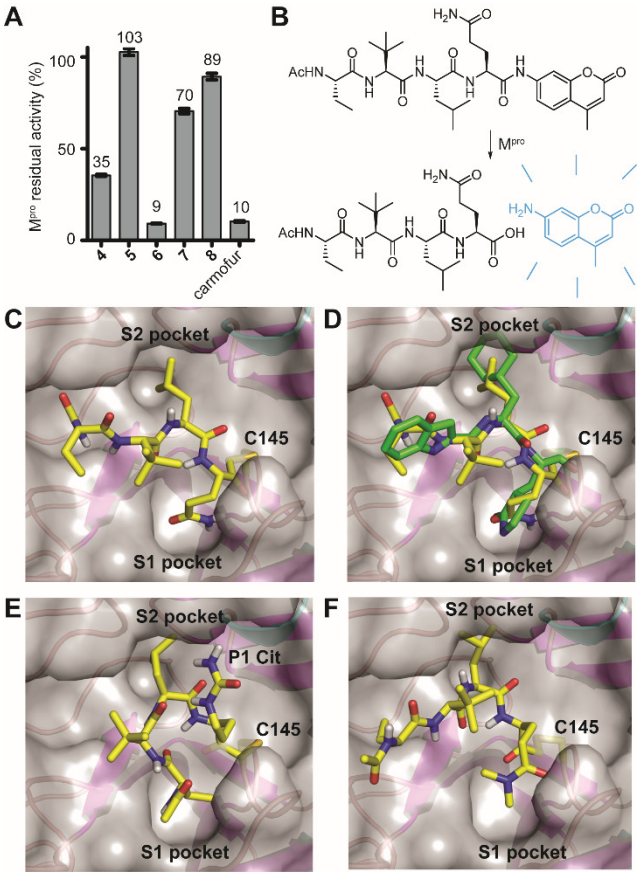

Figure 1: Active site inhibition of SARS-CoV-2 M^{pro}. (a) Bargraphs or residual activity after 1h incubation with 10 μM of indicated compound. (b) Utilized fluorogenic substrate. (c) Close-up of the SARS-CoV-2 M^{pro} (PDB code: 6LZE) with docked probe **4**. Protein is depicted as cartoons and a transparent surface (with β-sheets in magenta, helices in cyan and random coil in pink). The covalently bound inhibitors and the side chain of the active site C145 are drawn as sticks (in green). Pictures rendered in PyMol.[32] (D) Overlay of docked probe **4** with the original aldehyde inhibitor in the M^{pro} complex of PDB structure 6LZE. (E) Covalently docked probe **6** with P1 GlnMe$_2$ (in magenta) (F) Covalently docked probe **5** with P1 Cit. Note that the Cit side chain in P1 does not show an interaction with the S1 pocket.

Covalent labeling of SARS-CoV-2 M^{pro} – We assessed the ability of the most potent probes, **4** and **6**, to covalently label M^{pro}. Purified M^{pro} was incubated with different concentrations of probe **4** or **6** for one hour at 37 °C, after which either a TAMRA fluorophore or biotin was introduced as a detection tag by click chemistry (copper-catalyzed azide-alkyne cycloaddition).

In-gel fluorescence clearly shows that M^{pro} is covalently modified by both **4** and **6** at concentrations as low as 200 nM (Figure 2A). Biotin blot was also able to detect the covalent probe-Mpro complex, albeit with slightly lower sensitivity. Overall, probe **6** with the dimethyl-Gln in the P1 position is more sensitive than probe **4**, in line with the results from the inhibition assay. This may be attributed to the possible reversible formation of a cyclic hemiamidal by reaction of the glutamine side chain with the ketone (Figure 2B).

We next investigated the capacity of the probes to label SARS-CoV-2 M^{pro} in a complex proteome. To this end, prepared lysates of *E. coli* that were induced or not induced to express recombinant M^{pro}. Because the click chemistry could potentially be problematic in more complex samples, we also synthesized a pre-clicked TAMRA version of probe **4** (probe **9**; see Figure S2). Both probe **4** and **6** were able to label M^{pro} selectively in the bacterial lysate, as the few other observed bands were caused by click chemistry background labeling as judged from a no probe control sample (Figure 2C). Labeling by probe **4** and **6** is largely prevented by the active site inhibitor carmofur and no substantial labeling was observed in the lysates of uninduced bacteria. Both results demonstrate the selectivity of the probes.

For future application in infected human cells, we wanted to show that the probes do not show crossreactivity with human proteins. As we lack the facilities in our laboratory to work with live viruses, we spiked lysates of HEK293T cells with different amounts of purified M^{pro} and labeled with preclicked probe **9**. SDS-PAGE followed by fluorescent scanning revealed that M^{pro} was detected with a sensitivity down to 0.07% of the total proteome content. No other substantial gel bands were detected, illustrating that probe **9** specifically labels M^{pro} within a complete human proteome.

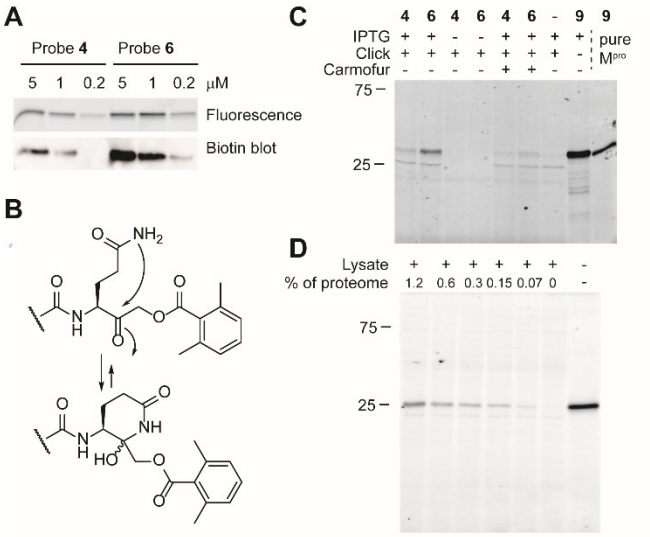

Figure 2. Covalent labeling of SARS-CoV-2 M^{pro} by ABPs. (a) Detection of purified recombinant M^{pro} by ABP **4** and **6** at 3 different concentrations, detected by fluorescent scanning of TAMRA fluorophore (upper panel) or biotin blot (lower panel). (b) A free glutamine residue in the P1 position of a ketone electrophile is in equilibrium with its cyclic hemiamidal. (c) Labeling of lysates of *E. coli* induced or uninduced for expression of recombinant M^{pro}. Note that addition of covalent M^{pro} inhibitor carmofur dramatically decreases labeling. (d) Labeling of decreasing amounts of recombinant M^{pro} in HEK293T lysates reveals sensitivity of probe **9** down to 0.07% of total proteome content.

Conclusion

In conclusion, we designed and synthesized different ABPs targeting the protease M^{pro} of SARS-CoV-2. They are based on cysteine reactive AOMK electrophiles and peptides resembling the substrate specificity of M^{pro}. AOMKs have not been reported before as inhibitors for M^{pro}. We have here demonstrated that they act as covalent, active site inhibitors. Admittedly, the P1 residues in this study are not yet optimal, as the side chain of Gln may form a cyclic hemiamidal and the $GlnMe_2$ is generally less favorable for M^{pro}. Hence, we anticipate that further optimization of the peptide element as well as the primed site leaving group will lead to AOMK probes and inhibitors with higher potency. Nevertheless, the here described probes are able to detect M^{pro} in complex proteomes without background labeling of other

proteins. This can be attributed to the lack of human proteases with preference for a P1 Gln. Because of this lack of crossreactivity, these probes will be useful tools for detection and visualization of target engagement of M^{pro} inhibitors in *in situ* infection models. We therefore expect that they will be well applicable in drug development studies against coronaviruses.

Acknowledgements

We thank Dr. Ladan Khodaparast and Dr. Laleh Khodaparast (Switch laboratory) for providing access to and help with the Avestin Emulsiflex, Prof. Rolf Hilgenfeld for kind donation of the plasmid for SARS-CoV-2 M^{pro} expression, Dr. Linlin Zhang for useful discussions on expression and purification, Peptides International for donation of the fluorogenic substrate, Prof. Wim De Borggraeve and Bart Van Huffel for NMR measurements, and Suravi Chakrabarty for providing HEK293T lysates. We acknowledge financial support from Research Foundation Flanders FWO (project number G0D8617N to SHLV and post-doctoral fellowship 12Y0720N to MBX), the Ministerium für Kultur und Wissenschaft des Landes Nordrhein-Westfalen, the Regierende Bürgermeister von Berlin–inkl. Wissenschaft und Forschung, and the Bundesministerium für Bildung und Forschung.

References

1. Tyrrell, D. A., and Bynoe, M. L. (1966) Cultivation of viruses from a high proportion of patients with colds, *Lancet 1*, 76-77.
2. Hamre, D., and Procknow, J. J. (1966) A new virus isolated from the human respiratory tract, *Proc Soc Exp Biol Med 121*, 190-193.
3. Kuiken, T., Fouchier, R. A., Schutten, M., Rimmelzwaan, G. F., van Amerongen, G., van Riel, D., Laman, J. D., de Jong, T., van Doornum, G., Lim, W., Ling, A. E., Chan, P. K., Tam, J. S., Zambon, M. C., Gopal, R., Drosten, C., van der Werf, S., Escriou, N., Manuguerra, J. C., Stohr, K., Peiris, J. S., and Osterhaus, A. D. (2003) Newly discovered coronavirus as the primary cause of severe acute respiratory syndrome, *Lancet 362*, 263-270.

4. Zaki, A. M., van Boheemen, S., Bestebroer, T. M., Osterhaus, A. D., and Fouchier, R. A. (2012) Isolation of a novel coronavirus from a man with pneumonia in Saudi Arabia, *N Engl J Med 367*, 1814-1820.

5. Zhu, N., Zhang, D., Wang, W., Li, X., Yang, B., Song, J., Zhao, X., Huang, B., Shi, W., Lu, R., Niu, P., Zhan, F., Ma, X., Wang, D., Xu, W., Wu, G., Gao, G. F., and Tan, W. (2020) A Novel Coronavirus from Patients with Pneumonia in China, 2019, *N Engl J Med 382*, 727-733.

6. Wang, C., Horby, P. W., Hayden, F. G., and Gao, G. F. (2020) A novel coronavirus outbreak of global health concern, *Lancet 395*, 470-473.

7. Thiel, V., Ivanov, K. A., Putics, A., Hertzig, T., Schelle, B., Bayer, S., Weissbrich, B., Snijder, E. J., Rabenau, H., Doerr, H. W., Gorbalenya, A. E., and Ziebuhr, J. (2003) Mechanisms and enzymes involved in SARS coronavirus genome expression, *J Gen Virol 84*, 2305-2315.

8. Ziebuhr, J. (2004) Molecular biology of severe acute respiratory syndrome coronavirus, *Curr Opin Microbiol 7*, 412-419.

9. Rawlings, N. D., Barrett, A. J., Thomas, P. D., Huang, X., Bateman, A., and Finn, R. D. (2018) The MEROPS database of proteolytic enzymes, their substrates and inhibitors in 2017 and a comparison with peptidases in the PANTHER database, *Nucleic Acids Res 46*, D624-D632.

10. Hegyi, A., and Ziebuhr, J. (2002) Conservation of substrate specificities among coronavirus main proteases, *J Gen Virol 83*, 595-599.

11. Chuck, C. P., Chow, H. F., Wan, D. C., and Wong, K. B. (2011) Profiling of substrate specificities of 3C-like proteases from group 1, 2a, 2b, and 3 coronaviruses, *PLoS One 6*, e27228.

12. Rut, W., Groborz, K., Zhang, L., Sun, X., Zmudzinski, M., Hilgenfeld, R., and Drag, M. (2020) Substrate specificity profiling of SARS-CoV-2 Mpro protease provides basis for anti-COVID-19 drug design, *bioRxiv*, 2020.2003.2007.981928.

13. Pillaiyar, T., Manickam, M., Namasivayam, V., Hayashi, Y., and Jung, S. H. (2016) An Overview of Severe Acute Respiratory Syndrome-Coronavirus (SARS-CoV) 3CL Protease Inhibitors: Peptidomimetics and Small Molecule Chemotherapy, *J Med Chem 59*, 6595-6628.
14. Hilgenfeld, R. (2014) From SARS to MERS: crystallographic studies on coronaviral proteases enable antiviral drug design, *Febs J 281*, 4085-4096.
15. Zhang, L., Lin, D., Sun, X., Curth, U., Drosten, C., Sauerhering, L., Becker, S., Rox, K., and Hilgenfeld, R. (2020) Crystal structure of SARS-CoV-2 main protease provides a basis for design of improved alpha-ketoamide inhibitors, *Science 368*, 409-412.
16. Jin, Z., Du, X., Xu, Y., Deng, Y., Liu, M., Zhao, Y., Zhang, B., Li, X., Zhang, L., Peng, C., Duan, Y., Yu, J., Wang, L., Yang, K., Liu, F., Jiang, R., Yang, X., You, T., Liu, X., Yang, X., Bai, F., Liu, H., Liu, X., Guddat, L. W., Xu, W., Xiao, G., Qin, C., Shi, Z., Jiang, H., Rao, Z., and Yang, H. (2020) Structure of M(pro) from SARS-CoV-2 and discovery of its inhibitors, *Nature*.
17. Dai, W., Zhang, B., Su, H., Li, J., Zhao, Y., Xie, X., Jin, Z., Liu, F., Li, C., Li, Y., Bai, F., Wang, H., Cheng, X., Cen, X., Hu, S., Yang, X., Wang, J., Liu, X., Xiao, G., Jiang, H., Rao, Z., Zhang, L. K., Xu, Y., Yang, H., and Liu, H. (2020) Structure-based design of antiviral drug candidates targeting the SARS-CoV-2 main protease, *Science*.
18. Sanman, L. E., and Bogyo, M. (2014) Activity-based profiling of proteases, *Annu Rev Biochem 83*, 249-273.
19. Chakrabarty, S., Kahler, J. P., van de Plassche, M. A. T., Vanhoutte, R., and Verhelst, S. H. L. (2019) Recent Advances in Activity-Based Protein Profiling of Proteases, *Curr Top Microbiol Immunol 420*, 253-281.
20. Cravatt, B. F., Wright, A. T., and Kozarich, J. W. (2008) Activity-based protein profiling: from enzyme chemistry to proteomic chemistry, *Annu. Rev. Biochem. 77*, 383-414.
21. Nomura, D. K., Dix, M. M., and Cravatt, B. F. (2010) Activity-based protein profiling for biochemical pathway discovery in cancer, *Nat Rev Cancer 10*, 630-638.

22. Sharifzadeh, S., Shirley, J. D., and Carlson, E. E. (2018) Activity-Based Protein Profiling Methods to Study Bacteria: The Power of Small-Molecule Electrophiles, *Curr Top Microbiol Immunol 420*, 23-48.

23. Desrochers, G. F., and Pezacki, J. P. (2019) ABPP and Host-Virus Interactions, *Curr Top Microbiol Immunol 420*, 131-154.

24. Rut, W., Groborz, K., Zhang, L., Modrzycka, S., Poreba, M., Hilgenfeld, R., and Drag, M. (2020) Profiling of flaviviral NS2B-NS3 protease specificity provides a structural basis for the development of selective chemical tools that differentiate Dengue from Zika and West Nile viruses, *Antiviral Res 175*, 104731.

25. Rut, W., Zhang, L., Kasperkiewicz, P., Poreba, M., Hilgenfeld, R., and Drag, M. (2017) Extended substrate specificity and first potent irreversible inhibitor/activity-based probe design for Zika virus NS2B-NS3 protease, *Antiviral Res 139*, 88-94.

26. Aleshin, A. E., Drag, M., Gombosuren, N., Wei, G., Mikolajczyk, J., Satterthwait, A. C., Strongin, A. Y., Liddington, R. C., and Salvesen, G. S. (2012) Activity, specificity, and probe design for the smallpox virus protease K7L, *J Biol Chem 287*, 39470-39479.

27. Kato, D., Boatright, K. M., Berger, A. B., Nazif, T., Blum, G., Ryan, C., Chehade, K. A. H., Salvesen, G. S., and Bogyo, M. (2005) Activity-based probes that target diverse cysteine protease families, *Nat. Chem. Biol. 1*, 33-38.

28. Zhang, H. Z., Zhang, H., Kemnitzer, W., Tseng, B., Cinatl, J., Jr., Michaelis, M., Doerr, H. W., and Cai, S. X. (2006) Design and synthesis of dipeptidyl glutaminyl fluoromethyl ketones as potent severe acute respiratory syndrome coronovirus (SARS-CoV) inhibitors, *J Med Chem 49*, 1198-1201.

29. Akaji, K., Konno, H., Mitsui, H., Teruya, K., Shimamoto, Y., Hattori, Y., Ozaki, T., Kusunoki, M., and Sanjoh, A. (2011) Structure-based design, synthesis, and evaluation of peptide-mimetic SARS 3CL protease inhibitors, *J Med Chem 54*, 7962-7973.

30. Jin, Z., Zhao, Y., Sun, Y., Zhang, B., Wang, H., Wu, Y., Zhu, Y., Zhu, C., Hu, T., Du, X., Duan, Y., Yu, J., Yang, X., Yang, X., Yang, K., Liu, X., Guddat, L. W., Xiao, G., Zhang,

L., Yang, H., and Rao, Z. (2020) Structural basis for the inhibition of SARS-CoV-2 main protease by antineoplastic drug Carmofur, *bioRxiv*, 2020.2004.2009.033233.

31. Bianco, G., Forli, S., Goodsell, D. S., and Olson, A. J. (2016) Covalent docking using autodock: Two-point attractor and flexible side chain methods, *Protein Sci 25*, 295-301.
32. Delano, W. L. (2002) The Pymol Molecular Graphics Systems (http://www.pymol.org).